Lidia M. Fontán, José L. Fernández, Ángel F. Doval, José L. Meniño, Cristina Trillo and J. Carlos López-Vázquez, "Wide-field, low-cost mapping of power ultrasound fields in water by time-average moiré deflectometry," in "Fringe 2013, 7th International Workshop on Advanced Optical Imaging and Metrology" Wolfgang Osten, Ed., 567-571, Springer-Verlag 2014

Wide-field, low-cost mapping of power ultrasound fields in water by time-average moiré deflectometry

Lidia M. Fontán[1], José L. Fernández[1], Ángel F. Doval[1], José L. Meniño[2], Cristina Trillo[1] and J. Carlos López-Vázquez[1]

[1]Departamento de Física Aplicada, Universidade de Vigo, Escola de Enxeñería Industrial, Campus Universitario, E36310 Vigo, Spain

[2]ANFACO-CECOPESCA, Carretera Colexio Universitario, 16, E36310 Vigo, Spain

1 Introduction

Characterization of acoustic fields in the power ultrasound range in water is a common problem in diverse application areas like sonochemistry, biomedicine, or industrial cleaning. Different approaches exist for the visualization and mapping of such acoustic fields, being a classical solution the mechanical scanning with pressure sensors (typically, hydrophones) over a grid of points [1]. For high intensity ultrasound, the analysis of bubbles trajectory has also been employed [2]. Alternative optical techniques are the scanning of a pointwise sensor (PIV, LDV) [3, 4], and also full field techniques like deflectometry or schlieren [5], smooth wavefront interferometry [6], holographic interferometry [7], ESPI and similar interferometric speckle techniques [4] or light diffraction tomography [8].

In spite of the wide variety of existing methods, most of them present shortcomings like the need of maintaining the acoustic field stable during the whole measurement process, or the sensitivity to environmental perturbations (very high for interferometric techniques) or the complexity, cost, fragility or lack of portability of the equipment, that may prevent making measurements in the field.

One of the well-known techniques to analyze phase objects is moiré deflectometry. This technique, developed in the nineteen-eighties [9], employs a well-shaped laser illumination (collimated or spherical) and two gratings to measure the deflections of the rays after passing through the object. Although its sensitivity in practical terms is smaller than that of interferometric techniques, when the observed acoustic fields have enough intensity, moiré deflectometry combines a sufficient sensitivity to the measurand with appropriate insensitivity to perturbations (environmental seismic and thermal effects, laser noise, etc.), with the additional benefit of covering a wide field of view (typically 30x30 cm^2) at a low cost, overcoming most of the aforementioned limitations.

We present the analysis by moiré deflectometry of the field in a water tank, produced by an exciter designed for ultrasonic cleaning. We developed the ex-

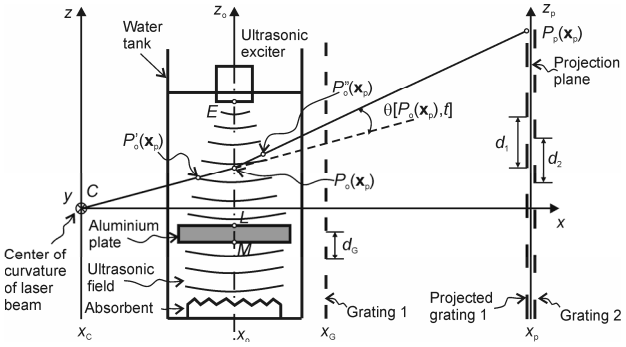

Fig. 1. Layout of the experimental system. A standing acoustic wave of fundamental frequency f=20 kHz produced by reflection on an aluminium plate is analyzed.

perimental system and a specific data processing procedure, based on the variations of the visibility of the moiré fringes by using the Fourier transform method.

2 Materials and methods

As the temporal spectrum of the excited wave is not monochromatic, we avoided stroboscopic techniques, choosing instead to record time-average images of the moiré pattern under CW illumination. Although this acquisition scheme loses the acoustical phase, we still retain information about the acoustic amplitude, which is enough for many practical engineering tasks.

We have adapted the paraxial model of moiré deflectometry under spherical illumination [10] to our particular configuration. The distances (Fig. 1) are named as $x_{op} = x_p - x_o$, $z_{LPo} = z_{Po} - z_L$, etc. Under the assumptions: (H1) Fresnel diffraction (which can be assumed if the pitch of the gratings is much larger than the optical wavelength), (H2) $x_{CG} >> y_{Gmax}$, z_{Gmax}, and (H3) $x_{CG} > 4\, x_{Gp}$, we obtained an expression of the time averaged intensity of the moiré pattern at the plane x_p

$$\left\langle I(\mathbf{x}_p,t)\right\rangle = I_c(\mathbf{x}_p)\left\langle 1+V(\mathbf{x}_p)\cos\left[\left(\mathbf{F}_1-\mathbf{F}_2\right)\mathbf{x}_p+\phi_1(\mathbf{x}_p,t)-\phi_2(\mathbf{x}_p)\right]\right\rangle \tag{1}$$

where $\mathbf{F}_j$ are the fringe vectors of the undistorted grids (i. e., the carriers) and ϕ_j are their phase distortion distributions. Specifically, for the projected grating 1:

$$\phi_1(\mathbf{x}_p,t) = \theta\left[P_o(\mathbf{x}_p),t\right]\frac{2\pi}{d_G}\left(\frac{x_{op}x_{CG}}{x_{Cp}}-x_{oG}\right) \tag{2}$$

being $\theta[P_o(\mathbf{x}_p), t]$ the instantaneous deflection angle of a generic ray passing through the point $P_o(\mathbf{x}_p)$ of the wavefield. In our application, Raman-Nath conditions apply and θ is proportional to the instantaneous pressure gradient [11]. The

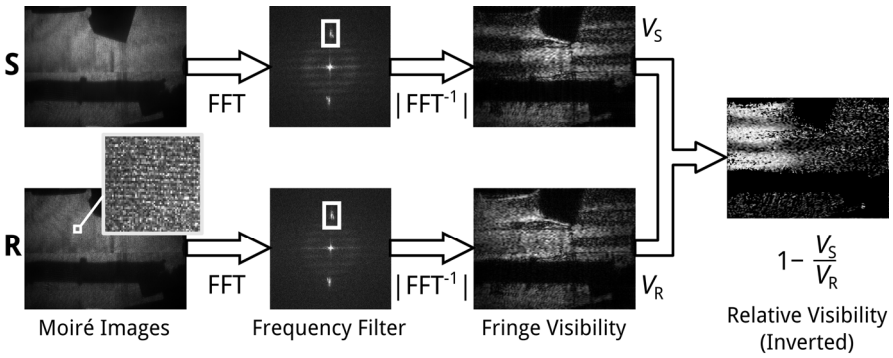

Fig. 2. Flow diagram of the fringe processing algorithm: (**S**) signal pattern (an acoustic wave is present in the field of view), (**R**) reference pattern (the fluid remains unaltered).

temporal dependence of this gradient is the cause of the reduction of the visibility of the pattern of Eq (1) in the areas where the gradient amplitude is greater.

As shown in Fig. 2, we calculate the visibility of the moiré patterns as the modulus of the complex amplitude returned by the Fourier transform method [12] (without translating the filtered spectrum to the origin of the frequency space). Though the changes induced by the presence of an acoustic wave become already apparent in these "visibility maps", we further improve their contrast by normalizing them with respect to the local maximum value of the visibility, obtained from a reference pattern (**R**) recorded with the fluid unaltered. We eventually invert the result, thus assigning the value "zero" to unaltered regions.

3 Results

An "inverted relative visibility" map obtained by using the proposed setup and data processing procedure is shown in Fig. 3. The moiré pattern was produced by using a 500 mW Nd:YAG laser and two laser-printed gratings; it was recorded with a 1392x1049 pixel camera and an exposure time of 300 ms.

An acoustic standing wave pattern can be noticed in the left hand side of the map. A graph of the rms pressure measured with a hydrophone along the centre of the acoustic beam is presented for comparison.

4 Acknowledgments

This work was funded by ANFACO-CECOPESCA in the framework of the project ECOSON; project code 10DPI014CT, Consellería de Economía e Industria, Xunta de Galicia", and by the UNIV. DE VIGO: "Láser de estado sólido", scientific equipment, FEDER 2003-04, exp. 15/2004, and contract number 12VI07.

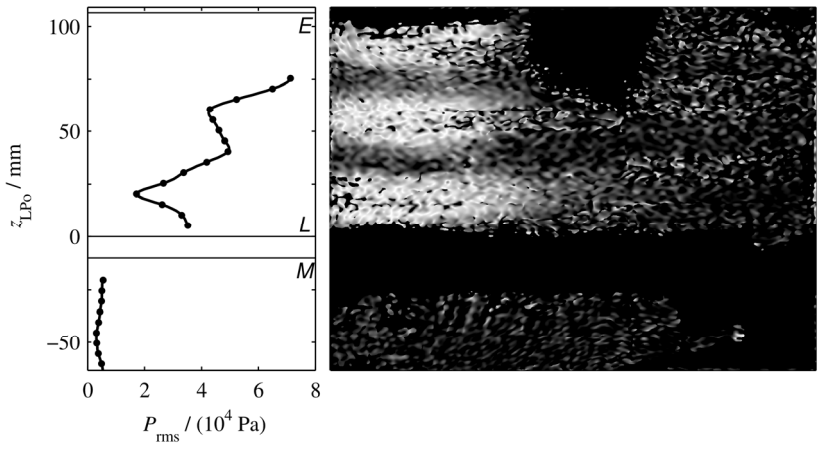

Fig. 3. Measured field of an acoustic wave. RMS pressure measured with a hydrophone along the axis z_o vs. moiré inverted relative visibility map yielded by the proposed technique.

References

1. Zhou, Y, Zhai, L, Simmons, R, Zhong, P (2006) Measurement of high intensity focused ultrasound fields by a fiber optic probe hydrophone. J. Acoust. Soc. Am. 120 (2):676-685
2. Gerfault, L, Cachard, C, Gimenez, G (1994) Mapping of an Acoustic Field by Analysis of Bubbles Trajectory. IEEE Ultrasonics Symposium:1363-1366
3. Longo, R, Vanherzeele, J, Vanlanduit, S, Guillaume, P. (2008) Underwater visualization of multi-input interleaved multisine wave fronts for ultrasonic testing of bones specimens using laser Doppler vibrometry. Proceedings of SPIE, vol. 7098:70980T
4. Mattsson, R (2006) Bending and acoustic waves in a water-filled box studied by pulsed TV holography and LDV. Optics and Lasers in Engineering 44:1146-1157
5. Schneider, B, Shung, K K (1996) Quantitative analysis of pulsed ultrasonic beam patterns using a Schlieren system. IEEE Trans. Ultrason. Ferroelectr. Freq. Control 43:1181-1186
6. Haran, M (1979) Visualization and Measurement of Ultrasonic Wavefronts. Proceedings of the IEEE, 67 (4):454-466
7. Hisada, S, Suzuki, T, Nakahara, S, Fujita, T (2002) Visualization and Measurements of Sound Pressure Distribution of Ultrasonic Wave by Stroboscopic Real-Time Holographic Interferometry. Jpn. J. Appl. Phys. 41 Part 1, No. 5B:3316–3324
8. Almqvist, M, Holm, A, Jansson, T, Persson, H W, Lindstrom, K (1999) High resolution light diffraction tomography: nearfield measurements of 10 MHz continuous wave ultrasound. Ultrasonics 37:343–353
9. Kafri, O, Glatt, I (1985) Moire deflectometry: a ray deflection approach to optical testing. Optical Engineering 24:944-960
10. Keren, E, Kafri, O (1985) Diffraction effects in moiré deflectometry. J. Opt. Soc. Am. A 2:111-120
11. Loeber, P, Hiedemann, E A (1956) Investigation of Stationary Ultrasonic Waves by Light Refraction. J. Acoust. Soc. Am. 28 (1):27-35
12. Takeda, M., Ina, H., Kobayashi, S. (1982) Fourier-transform method of fringe-pattern analysis for computer-based topography and interferometry. J. Opt. Soc. Am. 72(1):156-160